Accepted Manuscript

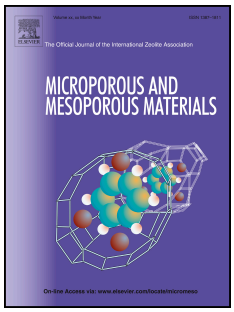

Enhancement of the hydrogenation activity of a Pd-tridecilamine (TDA) complex by confinement in carbon nanotubes

I. Such-Basáñez, M.C. Román-Martínez, P. Serp

PII: S1387-1811(16)00021-4

DOI: 10.1016/j.micromeso.2016.01.011

Reference: MICMAT 7523

To appear in: *Microporous and Mesoporous Materials*

Received Date: 23 November 2015

Revised Date: 8 January 2016

Accepted Date: 11 January 2016

Please cite this article as: I. Such-Basáñez, M.C. Román-Martínez, P. Serp, Enhancement of the hydrogenation activity of a Pd-tridecilamine (TDA) complex by confinement in carbon nanotubes, *Microporous and Mesoporous Materials* (2016), doi: 10.1016/j.micromeso.2016.01.011.

NT

H_2SO_4

$\varnothing_{in}$= 4-12nm

($\varnothing_{out}$=8-21 nm)

Ball Milled → NTBM

Air 773K → NTOx → (HCl) NTOxD

HNO_3 → NTN → (NaOH) NTN-ONa

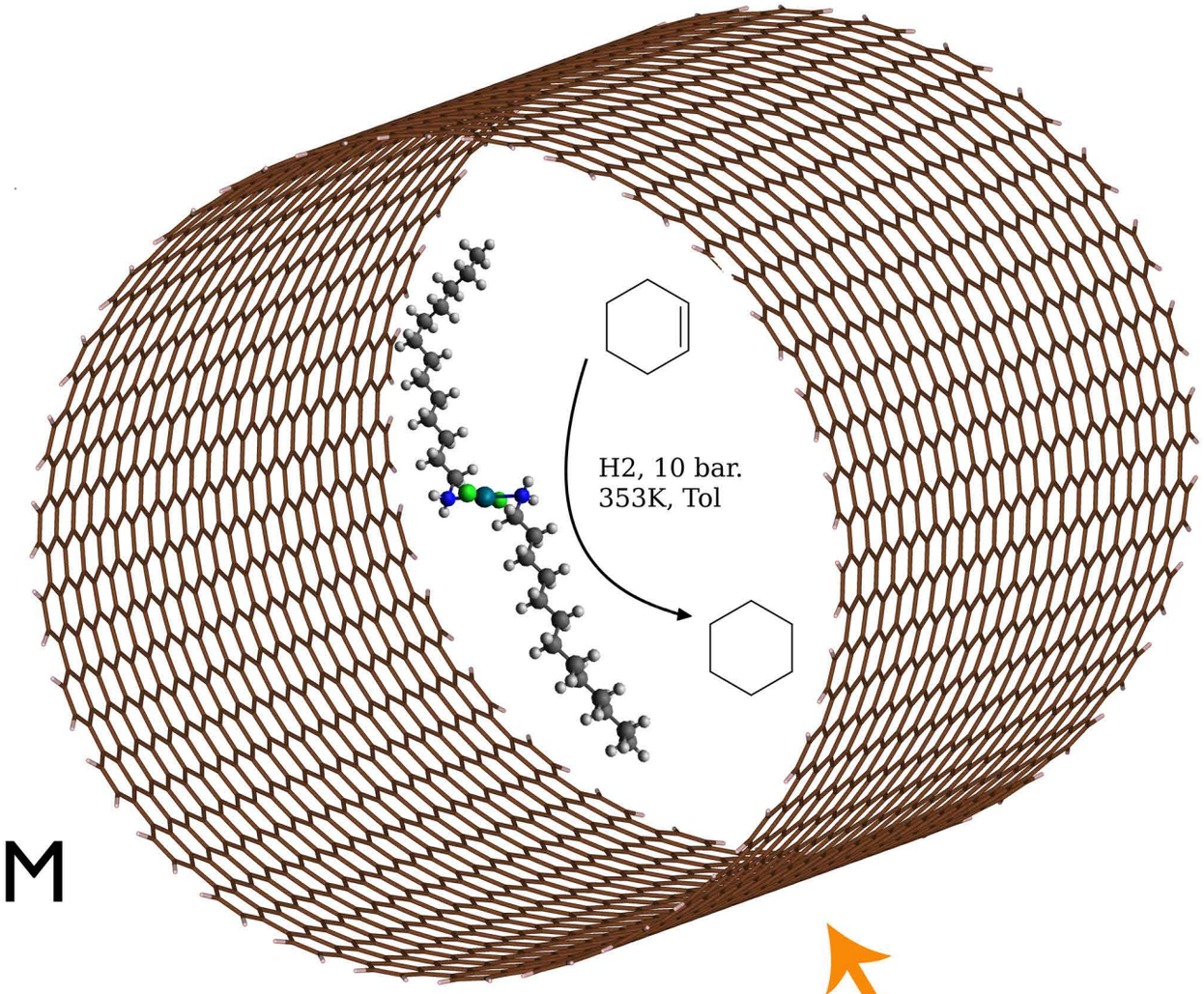

Enhancement of the hydrogenation activity of a Pd-tridecilamine (TDA) complex by confinement in carbon nanotubes

I. Such-Basáñez[a] * (Corresponding author)

[a]Department of Inorganic Chemistry and Materials Institute. University of Alicante (Spain).

ion.such@ua.es

M.C. Román-Martínez[a]

[a]Department of Inorganic Chemistry and Materials Institute. University of Alicante (Spain).

mcroman@ua.es

P. Serp[b]

[b]Laboratoire de Chimie de Coordination. CNRS-Université Toulouse (France).

Philippe.Serp@ensiacet.fr

Abstract

An active hydrogenation Pd complex has been immobilised by impregnation on CNTs submitted to several treatments that lead to important differences in their surface chemistry and in the proportion of tubes with both open ends. Most of the hybrid catalysts are more active than the complex in homogeneous phase, but the support properties have an important impact in the catalytic activity. In general, the more developed the surface chemistry, the lower the activity. However, when CNTs are open at both ends, Pd complex can enter the cavity of the tubes and an important enhancement of the catalytic activity due to a confinement effect is observed.

Keywords: Palladium; Hybrid Catalyst; carbon nanotube; hydrogenation; confinement.

1. Introduction.

* Present address: Technical Research Services. University of Alicante (Spain). Ap. 99 03080 - Alicante (Spain)

Homogeneous catalysts have played an important role in all areas of fine chemistry production as they are well known to be very active and selective under mild reaction conditions, an important factor to be taken into account when dealing with expensive organic substrates [1]. However, contrarily to heterogeneous catalysts, homogeneous catalysts lack the ability to be easily recovered from the reaction media. It would therefore be desirable to obtain a homogeneous catalyst immobilised on a solid support that could combine both, the high activity and selectivity of homogenous catalysts and the easiness of recovery of heterogeneous catalysts. Such system is often referred to as a hybrid catalyst, and it might give rise to other interesting properties like activity or selectivity enhancements due to the particular combination of metal complex and support. Researchers in this area of knowledge often seek this sort of synergistic effects.

Preparation of hybrid catalysts has been now thoroughly studied, as it is apparent from the literature [2–9]. A great variety of metal complexes and ligands, active and selective in a plethora of important reactions, have been immobilised on many different supports such as silica, zeolites, mesoporous ordered materials (MOMs), clays, polymers and carbon materials. Different anchorage methods have been explored mainly attending to the stability of the immobilisation. From this point of view, formation of a covalent bond between the homogeneous catalyst and the support has been the most used approach to this problem but other methods such as electrostatic or dispersive interactions cannot be overlooked. For example, a Pd complex with alkyl amine ligands was immobilised on active carbon materials by means of dispersive interactions by Díaz-Auñón *et al.*, showing that this procedure leads to stable and active hydrogenation catalysts [10].

Researchers have paid attention to the use of carbon nanotubes (CNTs) as catalyst support from the time of their discovery [11]. In particular, the characteristic shape factor of this material inspires its use as a drug delivery carrier [12] or, more related to catalysis, as a nanoreactor [13]. There are many examples of their use as catalyst support for the immobilisation of either homogeneous catalysts [8,11,14] or metal nanoparticles in the hollow cavity of nanotubes [15–18]. Previous work in our group showed that, in many cases, hybrid

catalysts based on CNTs are more active than analogous catalysts prepared with other carbon materials and this has been attributed to the confinement of the active species in the inner cavity of the nanotube [19–24]. Other researchers have also reported such effects when using metal-complex species [14,18,25,26]. The present work deals with the immobilisation of an active hydrogenation model catalyst on CNTs submitted to different treatments. Conditions to obtain stable immobilised catalysts by means of dispersive interactions on nanotubes will be discussed. In the course of this research an effect of the oxygen content of the support on the activity of hydrogenation catalysts was found and will also be analysed in this paper.

2. Experimental

2.1. Synthesis of complex *trans*-[$PdCl_2(NH_2$-$(CH_2)_{12}$-$CH_3)_2$] (PdTDA).

Preparation of *trans* square-planar PdTDA complex was described elsewhere [10] and can be summarized as follows: 100 mg (0.56 mmol) of $PdCl_2$ were added to a 50 mL toluene solution of 228 mg (1.1 mmol) of NH_2-$(CH_2)_{12}$-CH_3 (TDA), and the resulting suspension was heated to 338 K under flowing Ar for 4 h. The obtained yellow solution was evaporated and the product was purified by column chromatography (Acros 0.200-0.500mm; $CHCl_3$:CH_3OH 6:1), obtaining a yellow solid that was characterised by elemental analysis (Micro TruSpec LECO CHNS), ^1H and ^{13}C NMR (Bruker AV300), FTIR (Bruker IF66/S) and FT-Raman (Bruker RFS/100) spectroscopies. Characterisation shows that the expected complex has been prepared.

EA: C: 54.50 % (54.21 %); N: 4.54 % (4.86 %); H: 10.22 % (10.15 %).

^1H –NMR (300MHz): t 0.89 ppm (6H, C***H₃***); b 1.26 ppm (36H, internal C***H₂***); b 1.31 ppm (4H CH_2CH_3); m 1.66 ppm (4H C***H₂***CH_2NH_2), m 2.74 ppm (4H, C***H₂***NH_2), b 2.78 ppm (4H, N***H₂***).

^{13}C –NMR (300MHz): 14.1 ppm (CH_3); 22.7 ppm (***C***H_2CH_3); 26.5 ppm (***C***$H_2CH_2CH_2NH_2$); 7 signals between 29.1-29.7 ppm (internal ***C***H_2); 31.5 ppm (***C***$H_2CH_2CH_3$); 31.9 ppm (***C***$H_2CH_2NH_2$); 45.2 ppm (***C***H_2NH_2).

FTIR: 3250 cm^{-1}, d weak (N-H coordinated to Pd). The low number of multiple bands in the

spectrum suggests *trans* symmetry [27].

Raman: 3250 cm^{-1}, d weak (N-H coordinated to Pd); 288.5 cm^{-1}, s, medium, (Pd-N with contribution of Pd-Cl [28]).

2.2. Preparation and characterisation of supports.

Multiwall carbon nanotubes (MWCNT) were prepared at the Laboratoire de Chimie de Coordination (CNRS-Université Toulouse) using a metal growth technique over Fe particles [29], followed by a purification treatment with H_2SO_4 solution. The sample named NT, was characterised by TEM, revealing that the MWCNT present external diameters between 8 and 21 nm and inner diameters between 4 and 12 nm, which means that they have between 7 and 16 walls. Characterisation by gas adsorption techniques suggests that sample NT has one of its ends capped by the metal particle and a carbon shell, while the other end is open [21].
Sample NT was submitted to different treatments, which are schematically shown in Figure 1. Such treatments were: ball milling for 200 min (sample NTBM), air oxidation at 773 K for 1 hour (sample NTOx) and HNO_3 oxidation at room temperature (HNO_3 70%, 14 h) (sample NTN). Sample NTOx was further treated with HCl 5M (20 mL/g) at room temperature for 24 h in order to remove remaining metal impurities. Demineralised sample was named NTOxD. Sample NTN was treated with NaOH 0.25M (20 mL/g, 10 h, washing until pH 7) to develop sodium compensated anionic hydroxylate groups on its surface. This sample was named NTN-ONa.

Figure 1. Preparation of supports.

Ash content of CNT supports was measured by burning 1g of sample in a muffle furnace at 1173 K in air and determining the remaining weight.
Surface texture was characterised by gas adsorption isotherms (N_2 at 77 K and CO_2 at 273 K) measured in a Quantachrome Autosorb 6B instrument. Textural parameters were calculated

according to the procedure proposed by Rodríguez-Reinoso et al. [30]. Surface area was assessed from the N_2 adsorption isotherm by the BET method (S_{BET}). The total volume of micropores (V_μ) and the volume of micropores with diameters narrower than 0.7 nm ($V_{n\mu}$) were determined by applying the Dubinin-Radushkevich equation to the N_2 and CO_2 adsorption data, respectively. The difference V_μ-$V_{n\mu}$ is taken to be the volume of micropores with diameters between 0.7 and 2 nm ($V_{s\mu}$). Finally, the volume of N_2 adsorbed by the sample between p/p^0=0.2 and p/p^0=0.7 is used to calculate the volume of pores with diameters between 2 and 7.5 nm (V_{meso}).

Surface chemistry was assessed by X-Ray photoelectron spectroscopy (XPS) measured in a VG-Microtech Multilab 3000 using Mg Kα radiation with detector in constant energy mode at 50eV, and temperature programmed desorption (TPD) performed in a simultaneous TGA-DSC SDT 2960 coupled to a Pfeiffer ThermoStar mass spectrometer.

2.3. Preparation and characterisation of hybrid catalysts.

Most catalysts were prepared by the incipient wetness impregnation method as follows: 16.2 mg of the PdTDA complex were dissolved in 7 mL of toluene and slowly added over 1g of the nanotubes support (amounts to obtain 0.30 wt.% Pd); samples were left to dry overnight at RT and then vacuum dried at 333 K for 12 h. This preparation led to catalysts PdTDA/NT, PdTDA/NTBM, PdTDA/NTOx, PdTDA/NTOxD and PdTDA/NTN.

Searching for a more stable immobilisation of the catalyst supported on NTN-ONa, a different procedure was used: 1 g of support was suspended in a 20 mL methanol solution containing 16.2 mg of PdTDA, the mixture was stirred for 20 h at RT and then, the catalyst was filtered and thoroughly washed with methanol and toluene in order to remove ionic and weakly bound species. In this case, a more stable immobilisation by means of substitution of chloride ligands of the original complex by anionic moieties at the support's surface [29,31] is pursued. Figure 2 shows the design strategy for the preparation of catalyst NTN-O-PdTDA.

Figure 2. Preparation of catalyst NTN-O-PdTDA.

Pd content was measured by ICP-AES. The experimental method used to extract Pd from the catalyst was described elsewhere [32].

Catalysts were characterised by X-Ray photoelectron spectroscopy (VG-Microtech Multilab 3000) using Mg Kα radiation with detector in constant energy mode at 50 eV.

Sample NTN-O-PdTDA was also characterised by X-ray fluorescence in a Philips Magix Pro PW2400 spectrometer.

2.4. Catalytic activity measurements

Cyclohexene hydrogenation was carried out at 353 K using 30 mg of the hybrid catalyst, 10 mL of a 5 v/v% toluene solution of cyclohexene and 10 bar H_2 (S:C ratio was 5800) in a stainless steel, magnetically stirred (1100 rpm; no diffusion effects observed) Parr reactor (40 mL). Catalytic tests using the homogeneous PdTDA complex were also performed for comparison purposes. In this case, an amount of the metal complex of 0.49 mg was used (S:C=5800).

The reactor, loaded with the catalyst and the substrate solution, was purged five times with He and then purged with H_2. After setting the desired H_2 pressure, the reactor was introduced in the heating bath at 353 K.

After 20 h reaction time, the reactor was quenched using a water/ice bath, pressure released and reactor opened for analysis. The catalyst was removed by filtration, washed with toluene and stored under vacuum until the next reaction run. Following this procedure, three consecutive catalytic runs were carried out.

Analysis of reaction products was performed by gas chromatography (GC), using a HP6890 Series II chromatograph, with a HP-1 Methyl Siloxane capillary column, 30 m x 250μm x 0.25μm and a FID detector.

3. Results and discussion

3.1. Characterization of supports

3.1.1. Ash content

CNTs usually contain some residual metal particles coming from the catalyst used in their synthesis. In the present case, the catalyst used was iron and thus the ash after CNT combustion is iron oxide. Table 1 shows ash content of the analysed supports.

Table 1. Ash content of supports.

These data show that the different treatments performed to the pristine CNTs (sample NT) produce a reduction of the ash content. Ball milling and air oxidation treatments are likely responsible of the removal of tube caps and this could lead to the loss of some metal particles. The acid treatments present in samples NTOxD, NTN and NTN-ONa seem to remove tube caps and also to produce the dissolution, through iron oxidation, of the metal particles.

3.1.2. Porous texture

Figure 3 shows the N_2 adsorption isotherms obtained for the CNT supports. Isotherms are type IIb according to the IUPAC classification, they correspond to platelet like particles [33] and are indicative of capillary condensation. It is considered that porosity in MWCNTs consists mainly of the inner hollow cores and aggregated pores formed by interaction of isolated MWCNTs [34,35]. It can be observed that there are almost no differences between samples regarding their adsorption capacity, however N_2 adsorption isotherms of some samples show a hysteresis loop (see inset in Figure 3). This has been interpreted as these samples having a larger number of nanotubes with both ends open [21,35,36]. Samples showing this behaviour are: NTOxD, NTN and NTN-ONa, that is, those with the lowest ash content. This interpretation is further supported by TEM observation of selected samples (Figure S1 in supplementary material)

Figure 3. N_2 adsorption isotherms (77 K) of CNT supports.

CO_2 adsorption isotherms (not shown) are also very similar for all supports, indicating that they have a similar microporous structure.

BET surface area and pore volume distribution are presented in Table 2.

Table 2. Porous texture of supports

Data in Table 2 show that samples are very similar regarding their adsorption capacity and pore volumes. However, attending to the presence of hysteresis in the N_2 adsorption isotherm, the set of samples can be divided in two groups of different pore structure: NT, NTBM and NTOx, mainly with one open tube end, and NTOxD, NTN and NTN-ONa with a large amount of tubes with both ends open.

3.1.3. Surface chemistry

Figures 4a and 4b show, respectively, CO_2 and CO evolution, corresponding to the TPD profiles of the supports. Quantification of TPD profiles is presented in Table 3.

Figure 4. TPD profiles of carbon nanotube supports: a) CO_2 and b) CO.

Table 3. Surface chemistry of supports

CO TPD profiles of strongly oxidised samples (NTOx and NTN) show an intense peak at 1180-1200 K. Strong oxidation treatments lead to the transformation of remaining Fe used as catalyst in the CNT synthesis into iron oxide, which is reduced during TPD experiments by carbon from the nanotubes, explaining this peak in the CO profile. This contribution has not been taken into account in the CO amounts presented in Table 3.

TPD data shown in Figure 4 and Table 3 indicate that:

i) Ball milling process produces a mild oxidation of the CNTs, mainly producing CO desorbing surface oxygen groups (sample NTBM).

ii) Oxidation treatment with air produces some increase in the amount of surface oxygen groups, particularly of those desorbing as CO_2 (samples NTOx and NTOxD).

iii) Treatment with HNO_3 produces a noticeable oxidation of the support's surface with creation of both CO_2 and CO desorbing surface groups (sample NTN).

iv) Treatment of sample NTN with NaOH produces the reduction of the amounts of CO, and particularly, CO_2 desorbed (sample NTN-ONa). This means that the treatment with the basic solution leads to a significant modification of the surface chemistry, either by destruction of surface groups or by their transformation into species of higher thermal stability.

3.2. Characterisation of hybrid catalysts

Pd content of all fresh catalysts prepared by incipient wetness is 0.30 wt.%. This is an expected result because the preparation method assures that all the complex present in the impregnating solution remains on the support's surface; no cleaning procedure is applied. Sample NTN-O-PdTDA, that was prepared in excess methanol solution contains 0.26 wt.% Pd, an amount slightly less than the nominal amount (0.30 wt.%).

Table 4 shows XPS data obtained for selected catalysts PdTDA/NT, Pd/NTOxD and NTN-O-PdTDA. Excepting the case of this last sample, XPS analysis of the fresh hybrid catalysts reveals that the binding energy of Pd $3d_{5/2}$ as well as N/Pd and Cl/Pd atomic ratios are very close to those found for free PdTDA. Pd $3d_{5/2}$ binding energy is typical of a Pd(II) complex species [37,38] and a slight displacement (0.5 eV) is observed when compared to the free PdTDA complex. This reflects the fact that the interaction with the support has a slight electronic effect on Pd but the complex as an entity has not been modified (also supported by N/Pd and Cl/Pd atomic ratios). Pd/C atomic ratio in sample PdTDA/NTOxD is lower than in sample PdTDA/NT, therefore, it can be considered that a larger proportion of the Pd complex is located inside the nanotubes in sample PdTDA/NTOxD. As the wall thickness of the CNTs is

between 4 and 9 nm (i.e. 13 walls in average), photoelectrons coming from the Pd complex located inside the cavity are not expected to reach the XPS detector. XPS is usually quoted as being able to detect electrons coming from the outer 2 to 3 nm of the sample surface although actual detection depth depends on the inelastic mean free path of the electrons, which is a variable of different factors such as energy of the considered photoelectrons and material properties [39].

Table 4. XPS analyses of PdTDA complex and hybrid catalysts.

Under the analysis conditions used, neither Pd, N or Cl have been detected by XPS in catalyst NTN-O-PdTDA. This observation can be explained if we consider that all the Pd complex molecules are located inside the inner cavity of CNTs, a quite surprising result as we expected anionic oxygen groups to anchor this complex on the outer surface. Qualitative X-Ray Fluorescence Analysis and ICP analysis of fresh and spent catalysts have confirmed the presence of Pd in catalyst NTN-O-PdTDA, supporting the idea that all Pd must be inside the tubes in this catalyst. This results show that the strategy presented in Figure 2 has not worked as expected and therefore we did not achieve the immobilised species presented there.

According to these results, it seems that the presence of the complex only in the inner cavity of the nanotube happens when two conditions concur: i) the sample possesses a high proportion of nanotubes open at both ends and thus their filling with the PdTDA solution via nanocapillarity can occur [40] and, ii) the impregnation is carried out in excess solution and followed by thorough washing of the support.

This would explain why catalysts in which CNTs have both open ends but have been prepared by incipient wetness impregnation, the palladium complex is located both at the outer and at the inner surface of the tube while in catalyst NTN-O-PdTDA is selectively inside the CNTs. These observations will become apparent from catalytic activity measurements.

3.3. Catalytic activity

Table 5 shows cyclohexene conversion and TON (molecules converted per Pd atom) data obtained with the prepared hybrid catalysts and Pd complex in homogeneous phase.

Table 5. Cyclohexene conversion and TON values of homogeneous PdTDA complex and hybrid catalysts.

These data show that most of the hybrid catalysts are more active than the PdTDA complex in homogeneous phase. Besides, they hint an important effect of the support's properties, which can be related to both the support's surface chemistry and/or its porous structure.

To analyse the effect of surface chemistry, the catalytic activity of hybrid catalysts, as TON, has been plotted against the oxygen content of the supports (wt.% as determined by TPD). The plot, shown in Figure 5, allows arranging the data in two series: i) those of samples PdTDA/NT, PdTDA/NTBM and PdTDA/NTOx, and ii) those of samples PdTDA/NTOxD, PdTDA/NTN and NTN-O-PdTDA. It can be observed that in each of these two series, catalytic activity decreases with an increase of the support's oxygen content.

Figure 5. Cyclohexene conversion versus the oxygen content (wt.%) of the catalysts supports.

Catalysts PdTDA/NTOxD, PdTDA/NTN and NTN-O-PdTDA generally present a higher activity than the other catalysts. These more active catalysts are those in which the supports have been submitted to oxidative and acid treatments by which the ash content has been significantly reduced (see Table 1). In addition, and in close relation with the mentioned fact, the hysteresis loop that appears in the N_2 adsorption isotherms of these supports has been related to a larger amount of nanotubes with both ends open. Under these circumstances, the solutions of the complex used to prepare the catalysts by impregnation can more easily reach the inner cavity of the CNTs by nanocapillarity [40], leaving thus a certain amount of the active species located inside the tube. This confinement would, as previously reported [14,18–26],

enhance the catalytic activity, mainly due to an increased concentration of reactants inside the tube and close to the active species that compensates and even overcomes the diffusion limitations. Such a situation would be noticeably less likely in the case of CNTs capped at one end (catalysts PdTDA/NT, PdTDA/NTBM and PdTDA/NTOx).

A comparison of the catalytic performance of catalyst PdTDA/NTOxD with that of catalysts PdTDA/NTN and NTN-O-PdTDA reveals the mentioned negative effect of the support's surface chemistry. Such an effect can also be appreciated by comparing the TON of catalysts PdTDA/NT, PdTDA/NTBM and PdTDA/NTOx. This can be explained assuming that the more oxidized (polar) surface hinders the interaction with a low polarity reaction media and therefore the access of reactants to the active sites.

Confinement effect is made evident when comparing the behaviour of samples PdTDA/NTOx and PdTDA/NTOxD, in which both supports have a similar BET surface areas and similar surface chemistry but differ in the amount of nanotubes with both ends open, being the latter clearly more active.

A comparison of the TON of catalysts PdTDA/NT and PdTDA/NTN (entries 2 and 6 in Table 5) shows that both are similar in spite of the large difference in surface chemistry. In the case of sample PdTDA/NT none of the two mentioned effects: the positive confinement effect and the negative effect of a developed surface chemistry, play a significant role, while in the case of sample PdTDA/NTN they are balanced leading to an intermediate value of the catalytic activity.

Hybrid catalysts were tested in consecutive reaction runs to study their reusability. Figure 6 shows TON values in three consecutive runs, calculated with initial Pd loading. In this way, the potential activity loss is best appreciated.

Figure 6. TON of catalysts in consecutive reaction cycles

These data show that, in general, the catalytic activity decreases in consecutive runs, but such a decrease is much lower in the case of catalysts in which an important proportion of the

Pd complex is located inside the CNTs: PdTDA/NTOxD, PdTDA/NTN and NTN-O-PdTDA. The activity loss on reuse of catalysts PdTDA/NTOxD, PdTDA/NTN and NTN-O-PdTDA is low and thus, they can be considered reusable.

3.4. Study of spent catalysts

The amount of Pd in spent catalysts (after three consecutive runs) has been determined. The obtained data are shown in Table 6, where Pd loading of the fresh catalysts and the calculated leaching (as % of the original loading) have been also included.

Table 6. Pd loading (wt.%) of fresh and spent catalysts, and calculated Pd leaching (% of original loading).

Leaching is important in catalysts PdTDA/NT, PdTDA/NTBM and PdTDA/NTOx, meaning that in this case the Pd complex is not firmly immobilized on the support, most probably due to the fact that the complex is immobilized out of the cavity of the CNTs. Catalyst PdTDA/NTN presents an intermediate value of leaching while in catalysts PdTDA/NTOxD and NTN-O-PdTDA leaching is low, what is in agreement with a more stable anchorage due to the location of the metal complex in the inner cavity of the carbon nanotubes. The authors believe that complex immobilized on the outer surface of the nanotubes is easily leached from the catalysts, while the presence of PdTDA complex inside the cavity of the CNTs ensures its stability against leaching.

The observed decrease in catalytic activity (Figure 6) in consecutive catalytic runs can, therefore, be related to the loss of active species from one run to the next, being more noticeable in catalysts where only one open end is present.

XPS analysis of the used catalysts was not successful as the signals had a too low intensity or they did not appear, either because of the very low Pd loading in some used catalysts or because the remaining metal complex is located in the inner cavity of the CNTs as proposed above.

4. Conclusions

Hybrid catalysts have been prepared by the anchorage of the PdTDA complex on several CNT samples, which differ in their surface chemistry and in the proportion of tubes with both ends open. These properties of the support have shown to have an important impact in the properties of the hybrid catalysts.

Nanotubes with a developed oxygen surface chemistry lead to a lower catalytic activity, likely related with unfavorable interactions between the support and the reaction media (solvent and reactants).

Oxidized and/or acid treated CNTs have a larger proportion of nanotubes with both open ends and this allows the Pd complex to be located inside the nanotube cavity leading to a confinement effect by which the catalytic activity is enhanced. Besides, in this case, the anchorage is more stable and the catalysts are reusable.

Acknowledgements: The authors thank financial support by research projects MAT2012-32832 and PROMETEOII2014/010. Ion Such Basáñez wants to thank the staff of the X-Ray and Molecular Spectroscopy facilities at the University of Alicante Technical Research Services (SSTTI) for their help.

References

[1] J. Hagen, Industrial Catalysis: A Practical Approach, 2nd ed., Wiley-VCH, 2006.

[2] Z. Lu, E. Lindner, H.A. Mayer, Chem. Rev. (2002) 3543–3578.

[3] P. McMorn, G.J. Hutchings, Chem. Soc. Rev. 33 (2004) 108–122.

[4] R.A. Sheldon, Curr. Opin. Solid State Mater. Sci. 1 (1996) 101–106.

[5] A. Choplin, F. Quignard, Coord. Chem. Rev. 178--180 (1998) 1679–1702.

[6] C.E. Song, S. Lee, Chem. Rev. 102 (2002) 3495–3524.

[7] J.M. Thomas, R. Raja, Acc. Chem. Res. 41 (2008) 708–720.

[8] M.C. Román-Martínez, C. Salinas-Martínez de Lecea, in:, S. Suib (Ed.), New Futur. Dev. Catal. Hybrid Mater. Compos. Organocatalysts, Elsevier, ISBN: 978-0-444-53876-5, 2013, pp. 55–75.

[9] M.D. de la Torre, M. Melguizo-Guijarro, European J. Org. Chem. (2010) 5147–5154.

[10] J.A. Díaz-Auñón, M.C. Román-Martínez, C. Salinas-Martínez de Lecea, P.C. L'Argentière, E.A. Cagnola, D.A. Liprandi, M.E. Quiroga, J. Mol. Catal. A Chem. 153 (2000) 243–256.

[11] P. Serp, Appl. Catal. A Gen. 253 (2003) 337–358.

[12] B.S. Wong, S.L. Yoong, A. Jagusiak, T. Panczyk, H.K. Ho, W.H. Ang, G. Pastorin, Adv. Drug Deliv. Rev. 65 (2013) 1964–2015.

[13] A.N. Khlobystov, ACS Nano 5 (2011) 9306–9312.

[14] P. Serp, E. Castillejos, ChemCatChem 2 (2010) 41–47.

[15] O. Akhavan, M. Abdolahad, Y. Abdi, S. Mohajerzadeh, J. Mater. Chem. 21 (2011) 387–393.

[16] E. Castillejos, P.J. Debouttière, L. Roiban, A. Solhy, V. Martinez, Y. Kihn, O. Ersen, K. Philippot, B. Chaudret, P. Serp, Angew. Chemie - Int. Ed. 48 (2009) 2529–2533.

[17] T. Trang Nguyen, P. Serp, ChemCatChem 5 (2013) 3595–3603.

[18] X. Pan, X. Bao, Acc. Chem. Res. 44 (2011) 553–562.

[19] C.C. Gheorghiu, M.C. Román-Martínez, C. Salinas-Martínez de Lecea, ChemCatChem 5 (2013) 1587–1597.

[20] C.C. Gheorghiu, C. Salinas-Martínez de Lecea, M.C. Román-Martínez, Appl. Catal. A Gen. 478 (2014) 194–203.

[21] L.J. Lemus-Yegres, M.C. Román-Martínez, I. Such-Basáñez, C. Salinas-Martínez de Lecea, Microporous Mesoporous Mater. 109 (2008) 305–316.

[22] L.J. Lemus-Yegres, M.C. Román-Martínez, C. Salinas-Martínez de Lecea, J. Nanosci. Nanotechnol. 9 (2009) 6034–6041.

[23] M. Pérez-Cadenas, L.J. Lemus-Yegres, M.C. Román-Martínez, C. Salinas-Martínez de Lecea, Appl. Catal. A Gen. 402 (2011) 132–138.

[24] L.J. Lemus-Yegres, M. Pérez-Cadenas, M.C. Román-Martínez, C. Salinas-Martínez de Lecea, Microporous Mesoporous Mater. 139 (2011) 164–172.

[25] Y. Zhang, H.B. Zhang, G.D. Lin, P. Chen, Y.Z. Yuan, K.R. Tsai, Appl. Catal. AGeneral 187 (1999) 213–224.

[26] F. Yang, D. Deng, X. Pan, Q. Fu, X. Bao, Natl. Sci. Rev. 2 (2015) 183–201.

[27] P. Drözdzewski, E. Kordon, Vib. Spectrosc. 24 (2000) 243–248.

[28] P.C. L'Argentière, D.A. Liprandi, E.A. Cagnola, N.S. Fígoli, Catal. Letters 44 (1997) 101–107.

[29] R. Giordano, P. Serp, P. Kalck, Y. Kihn, J. Schreiber, C. Marhic, J. Duvail, Eur. J. Inorg. Chem. 4 (2003) 610–617.

[30] F. Rodríguez-Reinoso, A. Linares-Solano, in:, P.L. Walker (Ed.), Chem. Phys. Carbon, 1st ed., Dekker, 1988.

[31] A.R. Silva, C. Freire, B. de Castro, Carbon N. Y. 42 (2004) 3027–3030.

[32] J. Balué, J.C. Bayón, J. Mol. Catal. A Chem. 137 (1999) 193–203.

[33] F. Rouquerol, J. Rouquerol, K. Sing, Adsorption by Powders and Porous Solids. Principles, Methods and Applications., 1st ed., Academia Press, 1999.

[34] Q. Yang, P. Hou, S. Bai, M. Wang, H. Cheng, Chem. Phys. Lett. 345 (2001) 18–24.

[35] S. Inoue, N. Ichikuni, T. Suzuki, T. Uematsu, K. Kaneko, J. Phys. Chem. B 102 (1998) 4689–4692.

[36] J. Broekhoff, B. Linsen, in:, B.G. Linsen (Ed.), Phys. Chem. Asp. Adsorbents Catal., 1st ed., Academic Press, 1970.

[37] R. Benoit, Y. Durand, B. Narjoux, G. Quintana, Y. Georges, (n.d.).

[38] J. van den Berg, Surf. Interface Anal. 20 (1993) 1081–1082.

[39] J.F. Watts, J. Wolstenholme, An Introduction to Surface Analysis by XPS and AES, Wiley, 2005.

[40] D. Ugarte, A. Chatelain, W.A. de Heer, Science (80-.). 274 (1996) 1897–1899.

Table 1. Ash content of supports

Sample	Ash content (wt.%)
NT	4.0
NTBM	2.2
NTOx	2.3
NTOxD	0.8
NTN	0.8
NTN-ONa	0.5

Table 2. Porous texture of supports

Sample	S_{BET} (m^2/g)	$V_{n\mu}$ (cm^3/g)	$V_{s\mu}$ (cm^3/g)	V_{meso} (cm^3/g)
NT	259	0.04	0.05	0.11
NTBM	192	0.03	0.04	0.08
NTOx	224	0.03	0.05	0.10
NTOxD*	228	0.04	0.06	0.10
NTN*	227	0.04	0.06	0.09
NTN-ONa*	233	0.05	0.04	0.10

* Hysteresis loop in the N_2 adsorption isotherm (77 K)

Table 3. Surface chemistry of supports

Sample	CO_2 (µmol/g)	CO (µmol/g)	O (wt.%)
NT	151	137	0.7
NTBM	139	250	0.8
NTOx	228	195	1.0
NTOxD	215	230	1.1
NTN	506	703	2.7
NTN-ONa	229	542	1.6

Table 4. XPS analyses of PdTDA complex and hybrid catalysts.

Sample	Pd $3d_{5/2}$ (eV)	N 1s (eV)	Cl 2p (eV)	N/Pd	Cl/Pd	Pd/C_{CNT}
PdTDA	338.2	402.0	198.2	2.0	2.0	---
PdTDA/NT	337.7	402.0	198.1	1.9	1.9	0,00046
PdTDA/NTOxD	337.7	402.0	198.1	1.9	1.9	0,00029
NTN-O-PdTDA	n.d.	n.d.	n.d.	---	---	---

n.d. Not detected

Table 5. Cyclohexene conversion and TON values of homogeneous PdTDA complex and hybrid catalysts.

Sample	Conversion (%)	TON
PdTDA	10	584
PdTDA/NT	15	876
PdTDA/NTBM	7	408
PdTDA/NTOx	1	58
PdTDA/NTOxD	28	1696
PdTDA/NTN	12	700
NTN-O-PdTDA	11	736

Table 6. Pd loading (wt.%) of fresh and spent catalysts, and calculated Pd leaching (% of original loading).

Sample	Pd (wt.%) fresh catalyst	Pd (wt.%) spent catalyst	Pd leaching (%)
PdTDA/NT	0.30	0.10	67
PdTDA/NTBM	0.30	0.12	60
PdTDA/NTOx	0.30	0.09	70
PdTDA/NTOxD	0.30	0.25	16
PdTDA/NTN	0.30	0.19	37
NTN-O-PdTDA	0.26	0.22	15

Figure 1. Preparation of supports.

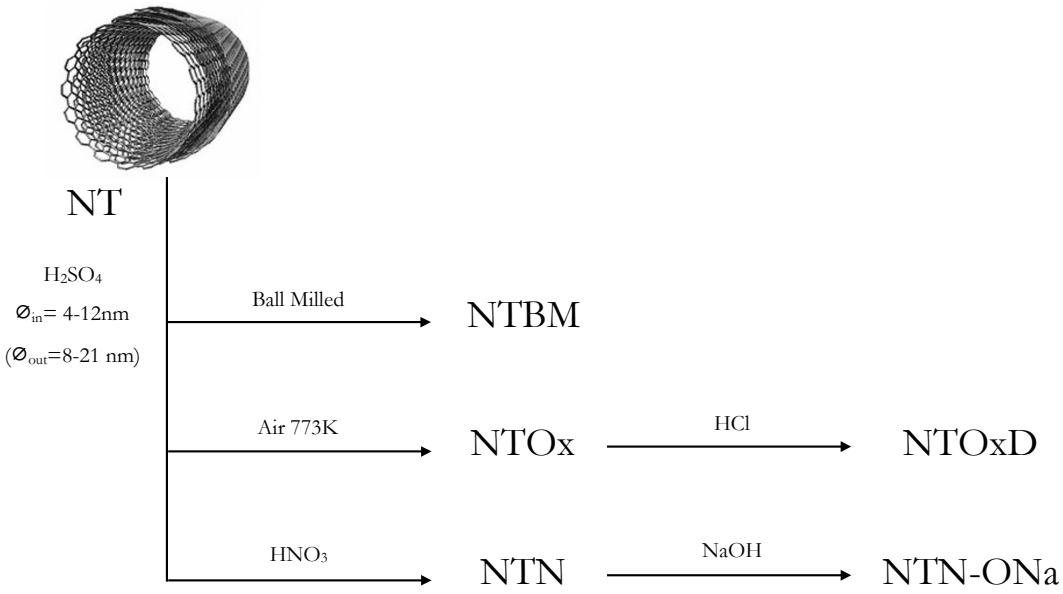

Figure 2. Preparation of catalyst NTN-O-PdTDA.

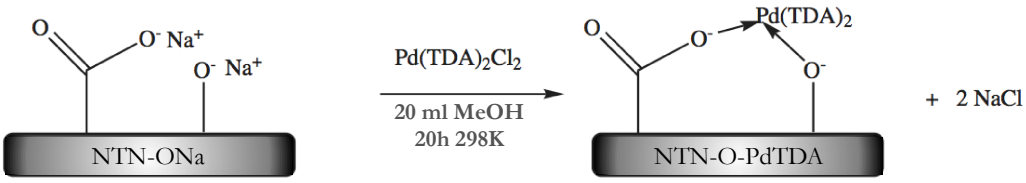

Figure 3. N_2 adsorption isotherms (77 K) of CNT supports

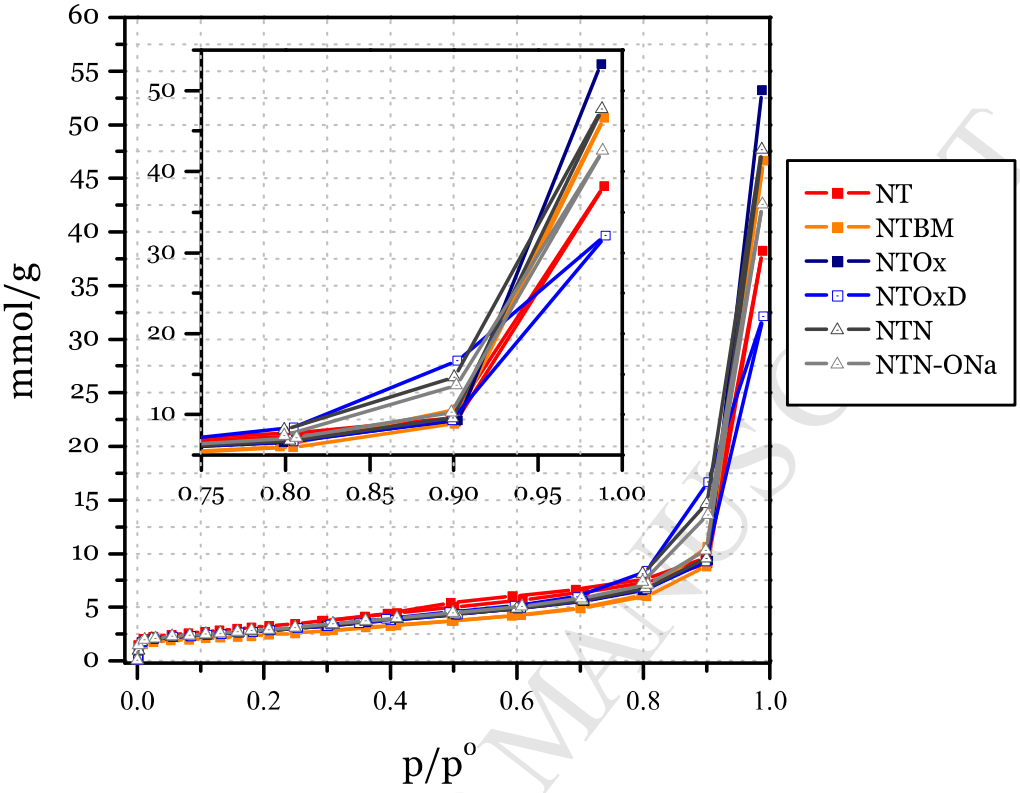

Figure 4. TPD profiles of carbon nanotube supports: a) CO_2 and b) CO.

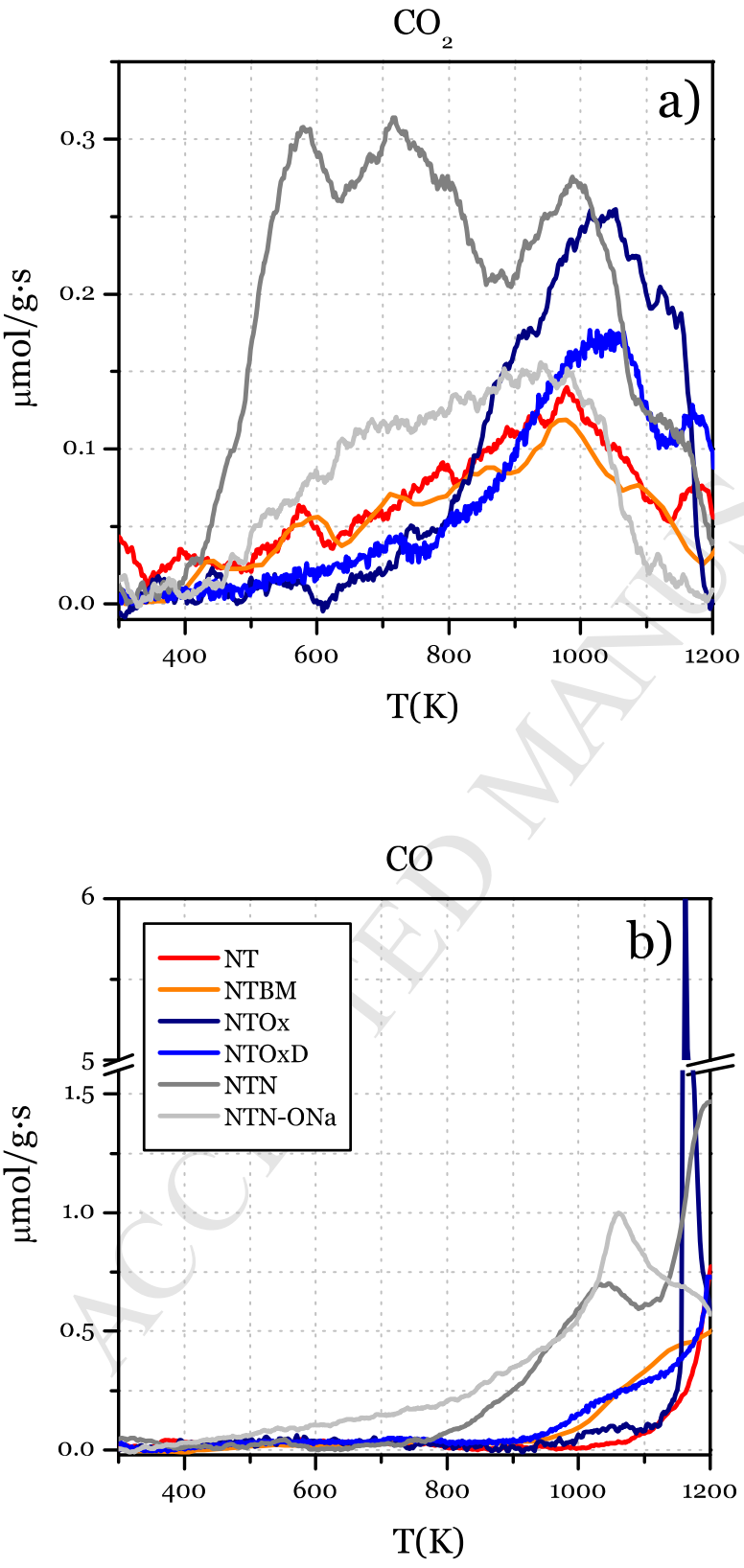

Figure 5. Cyclohexene conversion versus the oxygen content (wt.%) of the catalysts supports.

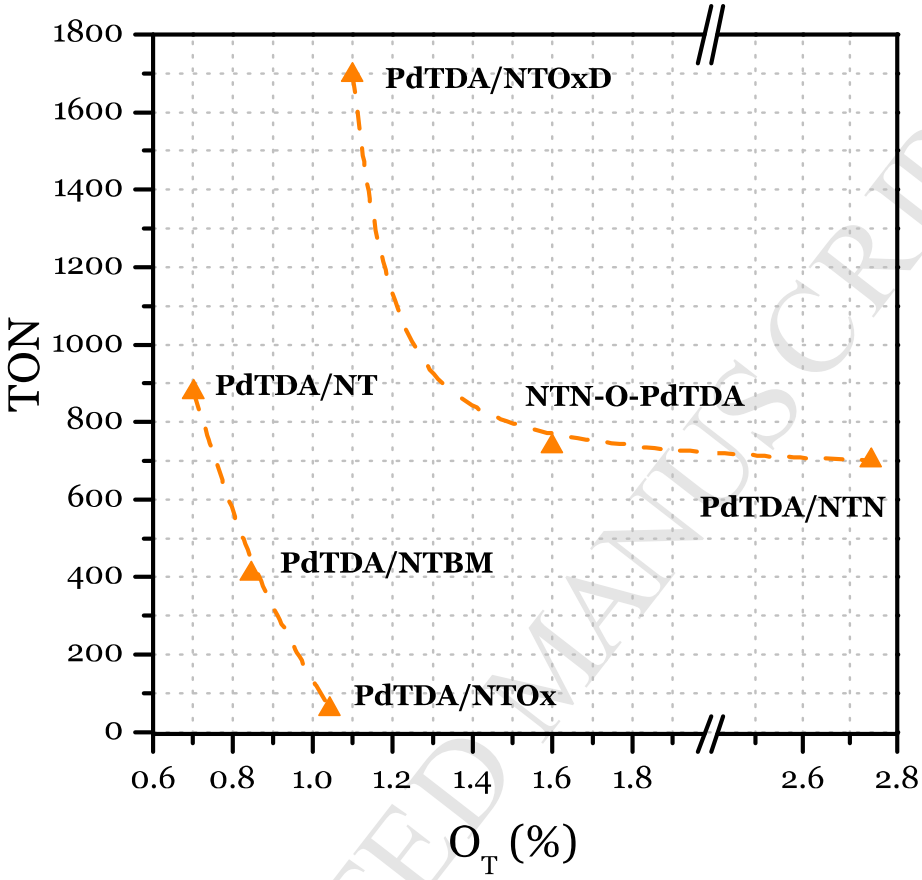

Figure 6. TON of catalysts in consecutive reaction cycles

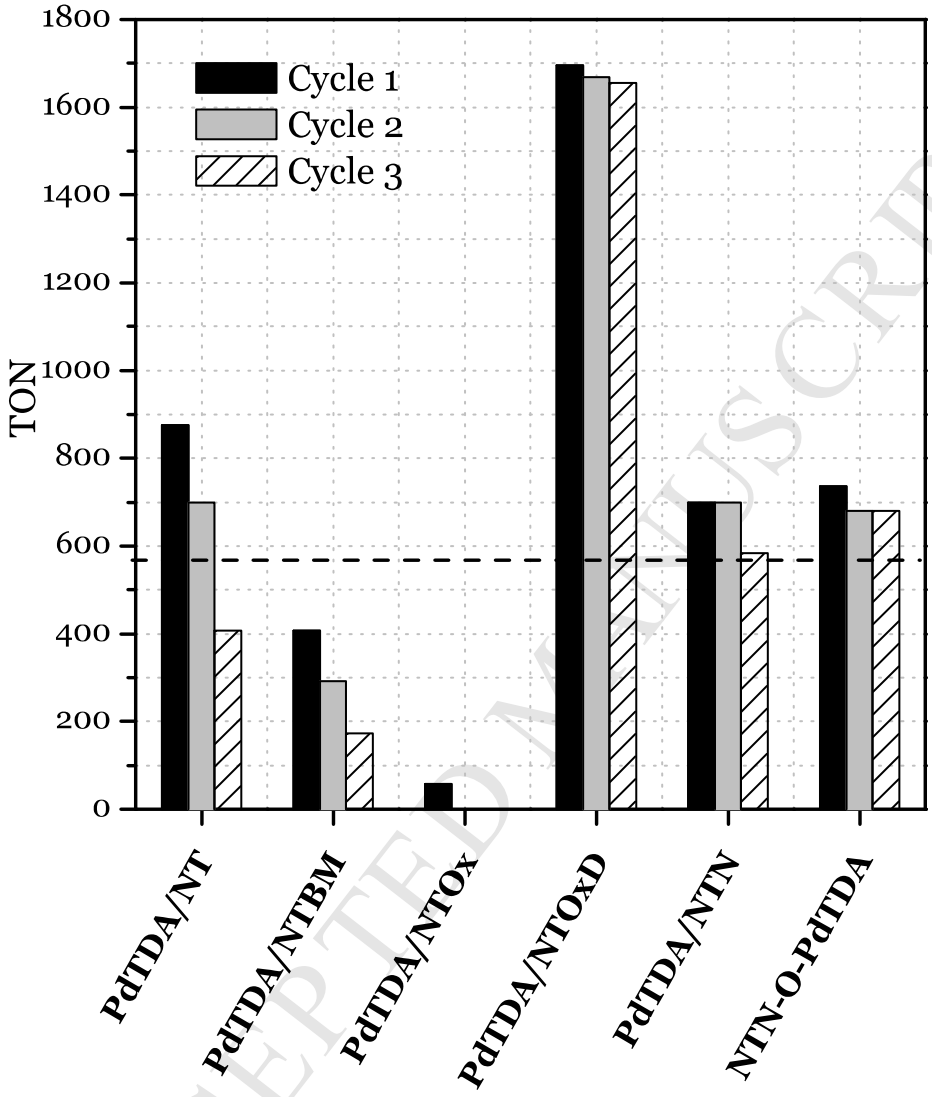

- Carbon nanotubes have been submitted to different chemical and physical treatments
- Acid treatment and oxidation remove residual metal and tube caps leading to both-ends open CNTs
- The PdTDA complex is mainly confined inside CNTs with both-ends open
- Confinement of the PdTDA complex leads to enhanced catalytic activity and stability